Negative differential resistance induced by thermalization of two-dimensional electrons in terahertz quantum-well photodetectors

X. G. Guo,[1,a)] L. L. Gu,[1] M. Dong,[1] J. C. Cao,[1] H. C. Liu,[2] and F. M. Guo[3]
[1]*Key Laboratory of Terahertz Solid-State Technology, Shanghai Institute of Microsystem and Information Technology, Chinese Academy of Sciences, 865 Changning Road, Shanghai 200050, China*
[2]*Key Laboratory of Artificial Structures and Quantum Control, Ministry of Education, Department of Physics, Shanghai Jiao Tong University, 800 Dongchuan Road, Shanghai 200240, China*
[3]*Key Laboratory of Polar Materials and Devices, Ministry of Education, East China Normal University, 500 Dongchuan Road, Shanghai 200241, China*

(Received 10 April 2013; accepted 16 May 2013; published online 31 May 2013)

Negative differential resistance (NDR) behavior existing in dark current-voltage (IV) curves of terahertz quantum-well photodetectors (QWPs) is theoretically investigated. Due to electron-electron scattering, the localized two-dimensional (2D) electrons in terahertz QWPs are thermalized. In steady state, the effective temperature of the 2D electrons is found to be higher than that of lattice. A self-consistent model is used to simulate the dark IV curves of terahertz QWPs, taking into account the thermalization effect of the 2D electrons. The NDR behavior is qualitatively reproduced. The periodic structures of electric-field domain and 2D electron occupation are formed in the NDR regime. The improved self-consistent model is useful for further understanding of the electron transport properties and improving the performance of terahertz QWPs. © *2013 AIP Publishing LLC*. [http://dx.doi.org/10.1063/1.4808343]

I. INTRODUCTION

Vertical electron transport across weakly coupled multi-quantum wells (MQWs) is a central issue for the performance improvement of quantum-well photodetectors (QWPs).[1] Recently, large current discontinuity and instability have been observed in the current-voltage (IV) curve of a terahertz QWP at a temperature of 1.5 K by Gomez *et al.*[2] Later, Delga *et al.* shown that the negative differential resistance (NDR) regime in the dark IV curve measured in a current sweeping mode was responsible for such current discontinuity and instability.[3] They concluded that the NDR was mediated by the space charge in the quantum wells (QWs) released by an intersubband impact ionization process;[4] and such depletion layers were near the emitter and collector contacts.

In QWPs, the impact ionization originates from the electron-electron (ee) interaction between the drift hot electrons in the continuum states above the QWs and the confined two-dimensional (2D) cold electrons in QWs.[4–6] In a more general point of view, the most important effect of ee interaction between the two groups of electrons is that the 2D cold electrons are thermalized. Therefore, in steady state, the effective temperature of the 2D electrons is higher than that of lattice. The temperature difference is determined by the densities and temperatures of the two groups of electrons, the escape probability of energetic 2D electrons, and energy exchange rate between 2D electrons and lattice. Because there are two degrees of freedom for the 2D electrons in QWs, it is expected that such energy exchange between the 3D hot electrons and the 2D cold electrons is efficient. The thermalization of 2D electrons has been found in quantum cascade lasers.[7] In terahertz QWPs, because the energy differences between the ground subbands and the continuum states are very small, the dark IV curves are very sensitive to temperature.[8] Therefore, it is necessary to consider the effect of 2D electron thermalization on the electron transport behaviors in terahertz QWPs.

II. THEORETICAL MODEL

Within a first-order approximation, the 2D electron effective temperature T_e can be expressed by the rate equation $dT_e/dt = S(E_k, J) - R(T_e, T_L)$, where $S(E_k,J)$ describes energy exchange rate between the 3D hot electrons and the 2D cold electrons, which is assumed to be proportional to the thermal power of the drift 3D electrons E_kJ with E_k the kinetic energy of a drift 3D electron in QW layers and J the current density, and $R(T_e,T_L)$ is the energy relaxation rate from the 2D electrons to lattice with T_L the temperature of lattice. In steady state, for a larger value of T_e, the increase of S will become slower and the energy relaxation rate R will be faster. Therefore, it is expected that there is a maximum value $T_{\max}$ for T_e. The kinetic energy of a drift electron in the ith QW layer is $E_{ki} = F_{i-1}v_d\tau + E_b - E_1$. Here, $v_d = uF_{i-1}/[1 + (uF_{i-1}/v_{sat})^2]^{1/2}$ is the drift velocity of electrons with F_{i-1} the electric field across the barrier on the left-hand side of the ith QW, μ the mobility, and v_{sat} the saturation drift velocity. Here, τ is the scattering time, E_b is the barrier height, and E_1 is the energy of the first subband bottom. In low temperature regime, the main energy relaxation channel from the 2D electrons to lattice is the electron-acoustic phonon scattering.[8] Therefore, the energy relaxation rate is $R(T_e, T_L) = A(T_e^\gamma - T_L^\gamma)$, where A and γ are two fitting parameters.[9] In steady state, the effective temperature T_{ei} of the 2D electrons confined in the ith QW is phenomenologically expressed as

a)Electronic mail: xgguo@mail.sim.ac.cn

$$T_{ei} = \begin{cases} \sqrt[\gamma]{T_L^{\gamma} + aE_{ki}J}, & \text{if } T_{ei} < T_{\max} \\ T_{\max}, & \text{if } T_{ei} \geq T_{\max} \end{cases}. \quad (1)$$

Here, a, γ, and $T_{\max}$ are three fitting parameters.

Due to Eq. (1), a positive feedback loop is introduced when the bias voltage is slightly increased at a critical bias point: larger current density → higher effective temperature of 2D electrons → more thermal emission of electrons from the QWs → larger current density. The positive feedback loop stops when T_e approaches to $T_{\max}$. The NDR regime can be qualitatively explained by the above positive feedback loop. In this paper, Eq. (1) is incorporated into a self-consistent model developed by Thibaudeau *et al.*[10] The numerical results show that the thermalization of 2D electrons in QWs can introduce NDR in dark IV curves of terahertz QWPs.

When a QWP is operated in steady state, the current J flowing through the device equals the injected current J_{inj} from the emitter contact (left end, electrons flowing from the left end to the right end of the device), and the number of captured electrons by one QW equals that of escape electrons from the QW.[10–13] Under the assumption of uniform electric field across each barrier, the dark IV relation is determined by the following coupled equations:[9]

$$\rho_i = \rho_d + \frac{\varepsilon_0 \varepsilon_r}{q}(F_i - F_{i-1}), \quad (2)$$

$$p_c J_{inj}(F_0, T_L, T_e) = J_{th}(\rho_i, F_i, T_e), \quad (3)$$

$$V = L_b F_0 + \sum_{i=1}^{N}(L_b + L_w)F_i, \quad (4)$$

where ρ_i is the 2D electron density in the ith QW, ρ_d is the Si doping density in the QWs, ε_0 is the vacuum permittivity, ε_r is the static dielectric constant, q is the electron charge, p_c is the electron capture rate, F_{i-1} (F_i) is the electric field across the left (right)-hand side barrier of the ith QW, J_{th} is the thermal emission and field-assisted tunneling current from the ith QW, V is the bias voltage applied to the device, N is the number of QWs, L_b is the barrier height, and L_w is the width of QW. The injected current J_{inj} is given by the following expression:[10,11]

$$J_{inj} = \frac{qm^* kT_L}{2\pi^2\hbar^3}\int_{E_c}^{\infty} T(E_z, F_0) \times \ln\left[\frac{1 + \exp((E_{Fc} - E_z)/kT_L)}{1 + \exp((E_{Fw} - E_z - qF_0L_b)/kT_e)}\right], \quad (5)$$

where m^* is the effective mass of electron, k is the Boltzmann constant, E_c is the energy of conduction band bottom, E_z is the electron kinetic energy along the direction of current flow, and E_{Fc} and E_{Fw} are the Fermi energies of the emitter contact and the first QW, respectively. Within the WKB approximation, the probability of tunneling $T(E_z,F_0)$ through the barrier is expressed as[9,10]

$$T(E_z, F_0) = \begin{cases} 1, & E_z \geq E_b \\ \exp[(-4/3qF_0)(2m^*/\hbar^2)^{1/2}(E_b - E_z)^{3/2}], & E_b - qF_0L_b \leq E_z < E_b \\ \exp[(-4/3qF_0)(2m^*/\hbar^2)^{1/2}(E_b - E_z)^{3/2} - (E_b - E_z - qF_0L_b)^{3/2}], & E_z < E_b - qF_0L_b \end{cases}. \quad (6)$$

The QWs are treated as three-dimensional emitters, and the thermal emission current J_{th} from the QWs is achieved by an expression similar with Eq. (5).

III. NUMERICAL RESULTS AND DISCUSSIONS

The studied terahertz QWP is labeled as V265 reported in Refs. 8 and 14. The MBE layers consist of a 400-nm top contact layer with Si doping of $1.0 \times 10^{17}/\text{cm}^3$, 40 quantum wells with $L_w = 11.9$ nm GaAs layers, $L_b = 55.2$ nm $Al_{0.05}Ga_{0.95}As$ barriers, and an 800-nm bottom contact layer doped with Si to $1.0 \times 10^{17}/\text{cm}^3$. The central 10-nm-wide region of each quantum well is Si doped to $\rho_d = 1.0 \times 10^{11}/\text{cm}^2$. The band structure of QW is obtained by solving the Schrödinger equation and Poisson equation with the exchange-correlation potential being considered in local density approximation.[2,15] Equations (1)–(6) are solved iteratively. The convergence criterion is that the maximum value of $|\rho_{i,n} - \rho_{i,n-1}|/\rho_d$ is less than 1.0×10^{-4} with n the nth iteration. The effective mass of electron is 0.067 m_0 with m_0 the electron mass. Because of a very small mole fraction of Al (0.05), the static dielectric constant of GaAs $\varepsilon_r = 10.88$ is taken in the following calculations. The barrier height is $0.84\,x = 0.042$ eV with x the Al mole fraction ratio.[10] The lattice temperature is $T_L = 4.0$ K. The electron mobility μ, the saturation drift velocity v_{sat}, the electron capture probability p_c, and the scattering time of drift electrons in the barrier layers are 5000 $\text{cm}^2/\text{V/s}$, 1.0×10^7 cm/s, 0.03, and 8.0 ps, respectively.

Fig. 1 shows the numerical dark IV curves and experimental data[3] in the inset. The fitting parameters are $a = 1.0 \times 10^{10}$, $\gamma = 4.0$, and $T_{\max} = 14$, 20, and 22 K. The main features of the NDR regime are reproduced qualitatively. The start point of the NDR regime is determined by parameters a and γ. The main features of NDR are characterized by parameter $T_{\max}$. For $T_{\max} < 15$ K, there is only a kink in the dark IV curve. With the increase of $T_{\max}$, the NDR regime appears and the magnitude of NDR-induced current discontinuity increases and the minimum bias voltages in the NDR regime approach to smaller values. Our model can reproduce the two-cusp shape of the NDR regime. Moreover, the transition point and the magnitude of current discontinuity can be well fitted by adjusting parameters a, γ, and $T_{\max}$. However, compared with the

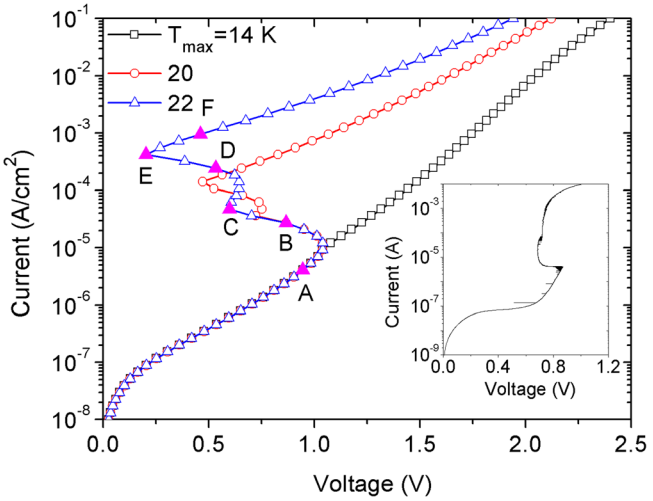

FIG. 1. Experimental and numerical dark IV curves of the terahertz QWP labeled as v265 in Refs. 12 and 13 at a lattice temperature of 4.0 K, the fitting parameters $a = 1.0 \times 10^{10}$, $\gamma = 4.0$, and $T_{\max} = 14$, 20, and 22 K. Inst: the experimental dark IV data.[3]

experimental data, our model gives much smaller values of the two minimum bias voltages at which the transitions of NDR states to positive differential resistance (PDR) states occur. Several reasons maybe responsible for such discrepancies. First, Eq. (1) is a phenomenological expression to describe the dependence of effective temperature on electric field and current density; more sophisticated method is needed. Second, the intersubband impact ionization is not included in our model. Finally, because of the accumulation and depletion of electrons in QWs in the NDR regime, the electron-related potential is significantly distorted; but such potential distortion is not considered in our calculations.

Fig. 2 presents the potential distributions for different injection current densities labeled as A, B, C, D, E, and F in the dark IV curve with $T_{\max} = 22$ K shown in Fig. 1. We find that the effective temperatures of 2D electrons in different QWs are different. Before the appearance of NDR transition (point A), the electric field across the main body of the

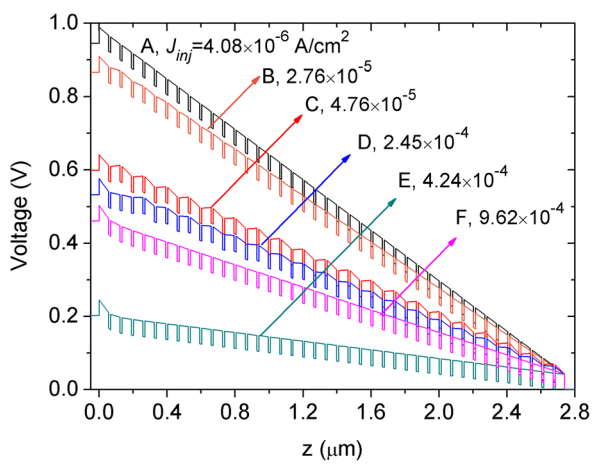

FIG. 2. Calculated electric potential distributions in the terahertz QWP of points A, B, C, D, E, and F shown in Fig. 1 with $T_{\max} = 22$ K. Hartree and Exchange-correlation potentials are not included.

device is uniform. According to Eq. (1), the effective temperature T_e has the same value for all the QWs. At point B near the beginning of the NDR regime, due to the increase of injection current, the electric field across the first barrier is larger than those across the other barriers. The flowing electrons in the first QW layer earn more energy from the electric field, which makes the 2D electrons in the first QW hotter. In steady state, since the current continuity must be satisfied, the electric field across the second barrier, and further the effective temperature of 2D electrons in the second QW become lower. For the same mechanism, the electric field across the third barrier increases. Therefore, at $J_{inj} = 2.76 \times 10^{-5}$ A/cm^2, electric-field domains are formed in the first three periods of the terahertz QWP. With further increasing injection current J_{inj}, the periodic electric-field domains are strengthened and they extend to the whole of the device. The period of the electric-field domains equals to twice of that of the MQW structure. Similar periodic field domain structure in mid-infrared QWPs has been reported by Ryzhii *et al.*[16] At the NDR-PDR transition point (C), the effective temperature T_e of 2D electrons in the odd number indexed (ONI) QWs equals to $T_{\max} = 22$ K. Because of over-thermal emission from the ONI QWs, the electric fields across the even number indexed (ENI) barriers are reversed. From point C to point D, the effective temperature T_e in ONI QWs equals to $T_{\max}$. Therefore, with the increase of injection current, the electric fields across the ONI barriers increase. At the same time, the effective 2D electron temperatures in ENI QWs increases, and the reversed electric fields across the ENI barriers decrease and approach to zero. So, in the C-D region, the dark IV shows PDR behavior. The second PDR-NDR transition near point D is triggered by the increase of effective 2D electron temperature in ENI QWs. At point E, the field domains are weakened because of the decrease of the effective temperature difference between the ONI QWs and the ENI QWs; the periodicity of the electric-field domains is smeared. Finally, the effective temperature T_e equals to $T_{\max}$ for all the QWs. The electric field across the main body of the terahertz QWP is uniform (Point F).

The numerical normalized total net electron density $\rho_T = \sum_{i=1}^{N}(\rho_i - \rho_d)/N\rho_d$ as a function of injected current is shown in Fig. 3. At the small injection current region, there is a small electron accumulation in the device. For $J_{inj} > 3.0 \times 10^{-7}$ A/cm^2, the device is electron depleted. The dip at point B originates from the thermalization of 2D electrons in ONI QWs. The sharp depletion of electrons in the D-E region is induced by the thermalization of 2D electrons in all QWs. As shown in the inset of Fig. 3 for point C, electrons are accumulated in ONI QWs and are depleted in ENI QWs. Similar with the structure of electric-field domain, the effective temperature difference between ONI QWs and ENI QWs introduces a periodic structure of 2D electron occupation in the QWs. Such periodicity is distorted with the decrease of the effective temperature difference (inset for point D). At point F, the effective temperature is $T_{\max} = 22$ K for 2D electrons in the MQWs. Near the emitter contact, there is a depleted layer consisting of four QWs. The other QWs are close to electrically neutral.

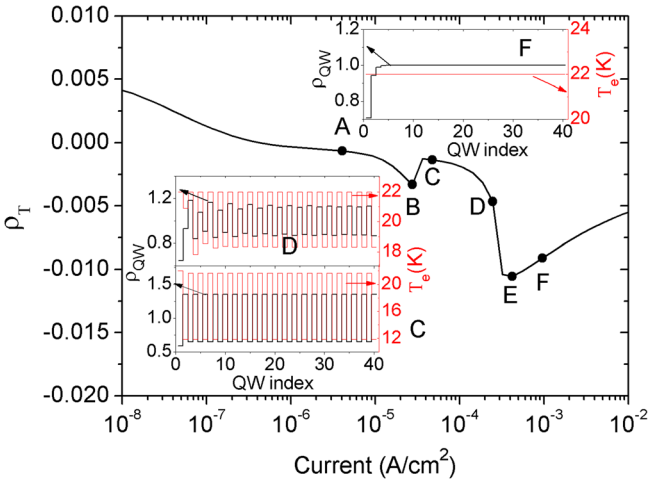

FIG. 3. Calculated normalized total net electron density ρ_T as a function of injected current. Inset: Numerical results of normalized electron density and electron temperature T_e in each QW ρ_{QW} for points C, D, and F shown in Fig. 1.

IV. CONCLUSIONS

In conclusion, we investigate the NDR properties existing in the dark IV curve of a terahertz QWP. A phenomenological expression is used to describe the current-induced thermalization of 2D electrons in the QWs. The main features of the NDR regime are reproduced. We find that the thermalization of 2D electrons is a two-step procedure. In the first step, the effective temperature of the 2D electrons in the ONI QWs reaches to T_{max}. In the second step, all the 2D electrons are completely thermalized. The periodic structures of electric-field domain and the 2D electron occupation are formed in the NDR regime.

ACKNOWLEDGMENTS

We thank Dr. A. Delga for providing us the experimental data shown in the inset of Fig. 1. This work was supported by the 863 Program of China (Project No. 2011AA010205), the National Natural Science Foundation of China (Grant Nos. 61176086, 61131006, and 60721004), the Major National Development Project of Scientific Instrument and Equipment (Grant No. 2011YQ150021), the Important National Science and Technology Specific Projects (Grant No. 2011ZX02707), the National Scientific Research Plan (2011CB932903), and the major project (Project No. YYYJ-1123-1), and the Hundred Talent Program of the Chinese Academy of Sciences. H.C.L. was supported in part by the National Major Basic Research Project (2011CB925603) and the Natural Science Foundation of China (91221201 and 61234005).

[1]H. Schneider and H. C. Liu, *Quantum Well Infrared Photodetectors: Physics and Applications* (Springer, New York, 2007).
[2]A. Gomez, V. Berger, N. Péré-Aapeme, and L. A. De Vaulchier, Appl. Phys. Lett. **92**, 202110 (2008).
[3]A. Delga, L. Doyennette, A. Buffaz, V. Berger, F. R. Jasnot, L. A. De Vaulchier, N. Péré-Laperne, and H. C. Liu, J. Appl. Phys. **110**, 013714 (2011).
[4]A. G. U. Perera, S. G. Matsik, V. Y. Letov, H. C. Liu, M. Gao, M. Buchanan, and W. J. Schaff, Solid-State Electron. **45**, 1121 (2001).
[5]L. Gendron, V. Berger, B. Vinter, E. Costard, M. Carras, A. Nedelcu, and P. Bois, Semicond. Sci. Technol. **19**, 219 (2004).
[6]S. Dong, N. Li, S. H. Chen, X. H. Liu, and W. Lu, J. Appl. Phys. **111**, 034504 (2012).
[7]R. C. Iotti and F. Rossi, Appl. Phys. Lett. **78**, 2902 (2001).
[8]H. C. Liu, C. Y. Song, A. J. SpringThorpe, and J. C. Cao, Appl. Phys. Lett. **84**, 4068 (2004).
[9]H. Celik, M. Cankurtaran, N. Balkan, and A. Bayrakli, Semicond. Sci. Technol. **17**, 18 (2002).
[10]L. Thibaudeau, P. Bois, and J. Y. Duboz, J. Appl. Phys. **79**, 446 (1996).
[11]E. Rosencher, F. Luc, P. Bois, and S. Delaitre, Appl. Phys. Lett. **61**, 468 (1992).
[12]H. C. Liu, Appl. Phys. Lett. **60**, 1507 (1992).
[13]B. F. Levine, J. Appl. Phys. **74**, R1 (1993).
[14]H. Luo, H. C. Liu, C. Y. Song, and Z. R. Wasilewski, Appl. Phys. Lett. **86**, 231103 (2005).
[15]X. G. Guo, Z. Y. Tan, J. C. Cao, and H. C. Liu, Appl. Phys. Lett. **94**, 201101 (2009).
[16]M. Ryzhii, V. Ryzhii, R. Suris, and C. Hamaguchi, Phys. Rev. B **61**, 2742 (2000).